DMD Fast Forward. Published on June 12, 2018 as DOI: 10.1124/dmd.118.080648
This article has not been copyedited and formatted. The final version may differ from this version.

Title Page

An investigation into the prediction of the plasma concentration-time profile and its inter-individual variability for a range of flavin-containing monooxygenase substrates using a physiologically based pharmacokinetic modelling approach

Authors:

Venkatesh Pilla Reddy, Barry C Jones, Nicola Colclough, Abhishek Srivastava, Joanne Wilson, and Danxi Li

Address:

Modelling and Simulation, DMPK, Oncology, IMED Biotech Unit, AstraZeneca, Cambridge UK, CB4 0WG (VPR)

DMPK, Oncology, IMED Biotech Unit, AstraZeneca, Cambridge UK (BCJ, NC & JW)

DSM, IMED Biotech Unit, AstraZeneca, Cambridge UK CB4 0WG (AS)

Pharmaron, Beijing, China, 100176 (DL)

DMD Fast Forward. Published on June 12, 2018 as DOI: 10.1124/dmd.118.080648
This article has not been copyedited and formatted. The final version may differ from this version.

Running Title Page

Running title: PBPK modelling of FMO substrates

Corresponding author: Dr. Venkatesh Pilla Reddy Ph.D

Address: Hodgkin Building c/o B310, Cambridge Science Park, Milton Road, Cambridge, Cambridgeshire, CB4 0WG, UK

Tel: +44 (0)7742645481

Email: venkatesh.reddy@astraneneca.com

No. of text pages: 39

No. of tables: 3

No. of figures: 4

No. of references: 38

Abstract word count: 286

Introduction word count: 545

Discussion word count: 868

Abbreviations: ADME, absorption, distribution, metabolism and excretion; ASA, automated sensitivity analysis (ASA); AUC, are under curve; Cmax, maximum concentration; CYP, Cytochrome P450; CL, clearance; CLint, intrinsic clearance; DIDB, Drug interaction database; FMO, flavin-containing monooxygenases; fu,P unbound fraction in plasma; fu,inc, unbound fraction in the incubation; Fm, fraction metabolized; HLM, human liver microsomes; IVIVE, in vitro/-in vivo extrapolation; LC-MS/MS, liquid chromatography-tandem mass spectrometry; Rb/p, blood/plasma ratio; rFMO, recombinant FMO; PBPK, Physiologically based pharmacokinetic; PK Pharmacokinetics. Vss, volume of distribution at steady state;

DMD Fast Forward. Published on June 12, 2018 as DOI: 10.1124/dmd.118.080648
This article has not been copyedited and formatted. The final version may differ from this version.

Abstract:

Our recent paper (Jones et al., 2017) demonstrated the ability to predict in vivo clearance of Flavin-containing Monooxygenases (FMO) drug substrates, using in vitro human hepatocyte and human liver microsomal intrinsic clearance (CL_{int}) with standard scaling approaches. In this paper, we apply physiologically based pharmacokinetic (PBPK) modelling & simulation approaches (M&S) to predict the clearance, AUC and C_{max} together with the plasma profile of a range of drugs from the original study. The human physiological parameters for FMO, such as enzyme abundance in liver, kidney, gut was derived from in vitro data and clinical pharmacogenetics studies. The drugs investigated include itopride, benzydamine, tozasertib, tamoxifen, moclobemide, imipramine, clozapine, ranitidine, and olanzapine. The fraction metabolised (Fm) by FMO for these drugs ranged from 21 to 96%. The developed PBPK models were verified with data from multiple clinical studies. An attempt was made to estimate the scaling factor for recombinant FMO (rFMO) using a parameter estimation approach and an automated sensitivity analysis (ASA) within the PBPK platform. Simulated oral clearance (CLpo), using in vitro hepatocyte data and associated extrahepatic FMO data, predicts the observed *in vivo* plasma concentration profile reasonably well and predicts AUC for all of the FMO substrates within 2-fold of the observed clinical data, while, 7 out of 9 compounds fell within 2-fold when human liver microsomal data was used. rFMO over-predicted the AUC by approximately 2.5-fold for 3 out of 9 compounds. Applying a calculated inter-system extrapolation scalar or tissue specific scalar for rFMO data resulted in better prediction of clinical data. PBPK M&S results from this study demonstrate that human hepatocytes and human liver microsomes can be used along with our standard scaling approaches to predict human in vivo PK parameters for FMO substrates.

Introduction

Flavin-containing monooxygenase (FMO) belong to a family of enzymes that oxygenate a wide variety of nucleophilic heteroatom-containing chemicals and drugs. FMO3 is the predominant functional isoform in adult human liver, while FMO1 and 5 are expressed in adult kidney and liver, respectively (Yeung et al., 2000). FMO enzymes can be differentiated from CYP enzymes via heat inactivation and selective substrate inhibition by methimazole (Cashman and Zhang, 2006; Taniguchi-Takizawa et al., 2015). There is a lack of validated methods for extrapolating in vitro hepatic intrinsic clearance (Clint) for FMO to in vivo clearance (IVIVE). Our earlier paper (Jones et al., 2017) investigated a set of 10 literature compounds with varying degrees of FMO involvement. The compounds were profiled in in vitro assays, which defined the extent of FMO involvement based on heat inactivation and inhibition by the selective substrate methimazole. The FMO contribution varied from 21% for imipramine to 96% for itropride. In addition, these data were used to predict the unbound intrinsic clearance and compared with human clearance data obtained from the literature. Using standard scaling scaled methods 70% of the compounds studied had predicted unbound intrinsic clearance within 2-fold of the observed unbound intrinsic clearance.

In this paper, we apply a mechanistic, physiologically based pharmacokinetic (PBPK) modelling & simulation approach (M&S) to predict the observed clinical data of drugs that are metabolized by FMO. The utility of PBPK modelling via a top-down approach (typically involving the estimation of the model parameters using observed clinical PK profiles) for FMO was shown for itopride (Zhou et al., 2017) which evaluated the impact of FMO3 polymorphism on exposure in Asian subjects. This study showed that genotyping for FMO3 to exclude subjects with homozygous Lys158/Gly308 alleles is not clinically relevant in terms of exposure and so not required. However, the elimination kinetics of itopride from in vitro studies using human liver microsomal (HLM) data resulted in about 8-fold under prediction of itopride clearance (Obach et al., 1997; Humphries et al., 2015; Zhou et al., 2017). This was similar to the FMO substrate benzydamine where under prediction was reported to be about 1.5 to 11-fold (Obach et al., 1997; Humphries et al., 2015; Zhou et al., 2017)). Thus, an additional

investigation to achieve a better in vitro/-in vivo extrapolation was warranted. As a result of the above observations, (Jones et al., 2017) generated in vitro data under well-defined experimental conditions. To date, there has not been a comprehensive assessment of FMO scaling using in vitro data and a bottom-up (typically, uses in-vitro data along with mechanistic understanding of ADME processes of drug to prospectively simulate the PK profiles) PBPK M&S approach for substrates with differing FMO contributions.

A human PBPK model, once established, can be a valuable tool to inform the clinical study design of an investigational drug under development, and help to link the exposure from healthy subjects to patients by taking into account pharmacogenetics and extrinsic factors or simulating the PK profiles in special populations such as paediatric subjects. Hence, the aim of this study was to investigate the performance of PBPK M&S to predict the concentration-time profiles, PK parameters (AUC, Cmax and CL), and inter-individual variability for a set of compounds for which all or part of the in vivo clearance has been determined to be mediated by FMO.

DMD Fast Forward. Published on June 12, 2018 as DOI: 10.1124/dmd.118.080648
This article has not been copyedited and formatted. The final version may differ from this version.

Materials and Methods

Compound selection and clinical data collection

Nine orally administered drugs namely itopride, benzydamine, tozasertib, tamoxifen, moclobemide, imipramine, clozapine, olanzapine and ranitidine were selected for PBPK modelling based on the availability of the in vitro and in vivo data within AstraZeneca or in the public domain. Clinical plasma profiles were digitized using an AstraZeneca internal tool namely, GI-SIM; (Sjogren et al., 2013) if literature data was used. Detailed clinical trial information for each of the nine drugs are described in Table 1. The PK data and parameters for these drugs were either extracted from the literature or obtained from internal clinical studies (e.g., tamoxifen).

PBPK Modelling Approach

Whole-body PBPK M&S of clinical PK data was performed using the population-based absorption, distribution, metabolism and excretion (ADME) simulator, Simcyp version 16 release 1 (Certara, Sheffield, UK; (Jamei et al., 2013)). The modeling assumptions and parameters were verified using clinical data for nine FMO substrates.

PBPK modelling input parameters

System-related parameters

Among the five FMOs, only FMO1, 3 and 5 are functional in human. FMO1 is a major form in human kidney (Yeung et al., 2000) while FMO3 and FMO5 are expressed mainly in liver (Dolphin et al., 1996; Koukouritaki and Hines, 2005). The reported FMO1 (kidney), FMO3 (liver) and FMO5 (liver) protein abundance values of 47, 71 and 22 pmol/mg protein were used in this analysis along with reported coefficient of variance (Haining et al., 1997; Overby et al., 1997; Yeung et al., 2000; Chen et al., 2016). Enzyme abundance, phenotype frequencies, and relative activities of FMO3 were accounted for within the virtual population of the simulator. The intrinsic catalytic activity per unit amount of FMO1 and FMO3 enzyme was assumed to be the same in healthy Caucasian, Japanese, and Chinese subjects as

the available expression data pool broadly represents the Caucasians and Asian population (Cashman and Zhang, 2006).

The Simcyp platform provides an enzyme kinetics pane for assessing the contribution to metabolic clearance in the liver, kidney or intestine for CYP and UGT enzymes, but not yet for FMOs. However, a user defined enzyme option, or unused UGT enzyme, within UGT enzyme kinetic pane allows entry of rFMO CL_{int} data, along with expression levels, frequency of polymorphism, turnover rate (Reddy et al., 2010) to define the FMO enzyme to enable IVIVE.

Drug-Related Parameters

The PBPK model input parameters used are listed in Table 2. The in vitro parameters such as CLint, plasma protein binding (Fu,P), fraction unbound in hepatocyte incubation (Fu,inc) were experimentally measured (Jones et al., 2017)., in some instances the PBPK platform's prediction toolbox was employed to predict the drug-related properties such as P_{eff} value using the mechanistic permeability model or the polar surface are/hydrogen bond donor (PSA/HBD) model if permeability data were not available. First order absorption rate constant (Ka) and fraction absorbed (fabs) were estimated from clinical data or predicted based on the P_{eff} value within the Simcyp simulator. Unless otherwise specified, the volume of distribution at steady state (Vss) for all compounds was predicted using the Rodgers and Rowland method (Rodgers et al., 2005; Rodgers and Rowland, 2006) within the PBPK simulator. Fraction unbound in microsomes and hepatocytes (Fu,mic and Fu,inc) was also included in the model.

Intrinsic Clearance Measurement using Hepatocytes and Human Liver Microsomes:

The measured *in vitro* data are detailed in Supplementary Table 1 and for methodology refer Jones et al, (Jones et al., 2017). The assignment of FMO metabolic intrinsic clearance and methodology employed to assess drug elimination are shown Supplementary Table 2.

Intrinsic Clearance Measurement in recombinant FMO1, FMO3 and FMO5 (rFMO1, rFMO3 and rFMO5):

DMD Fast Forward. Published on June 12, 2018 as DOI: 10.1124/dmd.118.080648
This article has not been copyedited and formatted. The final version may differ from this version.

The compounds (final concentration 1 µM) were incubated with rFMO1, 3 and 5 (final concentration 0.5 mg/ml protein). Incubations were carried out in duplicate in 100 mM potassium phosphate buffer (pH 7.4) containing NADPH (1 mM) in a total volume of 0.2 ml. Incubations were commenced with the addition of NADPH and carried out in a 96-well plate at a temperature of 37°C. At times ranging between 0 and 50 minutes, aliquots (0.02 ml) were removed and added to 0.08 ml of termination solution (acetonitrile + formic acid) containing buspirone (4nM) as an internal standard. Samples were vortexed, centrifuged at 3500 rpm for 5 minutes and the resulting supernatant was collected for liquid chromatography-tandem mass spectrometry (LC-MS/MS) analysis as shown in Supplementary Text and Supplementary Table 5.

Estimating the tissue specific scalar or intersystem extrapolation factor (ISEF) for extrapolation using recombinant FMO (rFMO) data

Human PK predictions using PBPK models and in vitro assays such as hepatocytes or HLM data combined with the appropriate scalars appears to be robust for CYP enzymes (Wagner et al., 2015; Luzon et al., 2016). However, very limited knowledge of scaling factors exists for drugs that are metabolized by non-CYPs such as FMOs. A drug-specific ISEF value can be derived using a formula shown below and in (Supplementary Table 1).

$$ISEF = \frac{CLint,u\ in\ HLM\ (\frac{\frac{ul}{min}}{mg}) \Big/ HLM\ FMO\ abundance\ (\frac{pmol}{mg})}{CLint,u\ in\ rFMO\ (\frac{ul}{min}{pmol})} \quad Eq\ (1)$$

When developing a model based on the rFMO data, the elimination via FMO1, FMO3, FMO5 enzymes were considered separately along with respective liver, kidney and intestine expression levels. The intrinsic catalytic activity per unit amount of FMO1, FMO3 and FMO5 enzymes were 71 pmol/mg protein in liver, 47 pmol/mg protein in kidney and 22 pmol/mg protein in intestine to reflect the

abundances of FMO3, FMO1 and FMO5, respectively. These abundance values were included in the population file using unused UGT enzyme with an user-defined option within Simcyp (Supplementary Table 2). The impact of FMO3 polymorphism was included in the final PBPK model. The remaining metabolic CL was accounted via major metabolizing enzymes of the drug via HLM in enzyme kinetics or via rCYP if CYP contribution is known as shown in the Table 2.

The automated sensitivity analysis (ASA) or parameter estimation (PE) option within Simcyp was utilized to determine the tissue specific rFMO scalar in liver, intestine and kidney tissue or to determine ISEF value. To this end, we used clinical data of the drugs that are mainly metabolized by FMO such as itopride. When the PBPK model was optimized to the clinical data of itopride using the ASA approach, the lower and upper bounds provided for the rFMO scalar parameter were 0 to 100 and used log-distributed step size with 10 steps (increasing with increased parameter value) within the Simcyp PBPK platform. The effect of the rFMO scalar on the C_{max}, AUC, CL and PK profiles were reviewed to understand the elimination trends of a drug. In addition to ASA, PE was performed using the weighted least square objective function to allow fitting to mean profile. Weighting by the reciprocal of the prediction was used as this provides a good fit for both C_{max} and the terminal phase when oral data is fitted to the model. The Nelder-Mead fitting algorithm was used with the default settings (reflection coefficient =1, expansion coefficient =2, contraction coefficient =0.5, and shrink coefficient =0.5).

PBPK Model Verification

PK simulations were conducted during the PBPK model development as a verification step to ensure appropriate model input parameters were used. The predicted PK parameters and simulated concentration-time profiles were compared with those observed in clinical trials (Table 1). The same trial designs as the clinical studies (e.g. dose, number of subjects, age, gender, population etc.) were used in the simulations. When a specific population was not available in the Simcyp simulator, for example for the Korean population, an alternative validated population such as the Japanese

population was used instead. In the case of olanzapine and clozapine, we assumed no difference between healthy subjects and patients as no validated schizophrenic population was available.

In addition to verification of PK parameters and PK profiles, we also investigated the nature of the correlation between human in vitro and in vivo clearance predicted by the PBPK approach using hepatocyte, HLM and rFMO data with ISEF and tissue specific scalars.

Results

PBPK Model Development and Optimization of PBPK Models

The plasma concentration profiles for nine orally or IV administrated FMO substrates were simulated by PBPK modelling using the hepatocyte CL_{int} data and compared with those observed clinically are shown in Figure 1. By visual inspection, the developed PBPK models adequately simulated the observed clinical data and so it was assumed that the models reflect the metabolic routes of elimination based on *in vitro* hepatocyte or HLM data (Figure 2), along with any known additional pathways like renal or biliary clearance. The observed and model simulated PK parameters such as AUC, C_{max} and CL are shown in Table 3. Table 3 shows that using hepatocyte intrinsic clearance (CL_{int}) data the PBPK model successfully predict AUC and Cmax for all 9 drugs within a factor of 2 compared to the clinical data. When HLM CL_{int} data was utilised 7 out of 9 drugs have these parameters correctly predicted within a factor of 2 (Supplementary Table 3 and Figure 2). Use of rFMO CL_{int} data over or under predicted the observed clinical data for 5 out of 9 compounds as depicted in the Forest plot using AUC as an end point (Figure 2) when no tissue specific factor (zero value) or ISEF option was used. The drug- specific ISEF values for each of the rFMO isoform determined using equation 1 are shown in Supplementary Table 1.

Based on ASA and PE analyses using itopride clinical data, an rFMO tissue scalar value of 0.2 or a compound specific ISEF appears to be reasonable value to obtain a good IVIVE as shown in Figure 3. Performance of the tozasertib PBPK model with an rFMO scalar value is shown as an example in Figure 3. Figure 3A, 3B and 3C show the model fit to observed data without and with ISEF or tissue scalar for itopride, while Figure 3D, 3E and 3F show the model fit without and with ISEF or rFMO scalar for tozasertib, respectively. This generic scalar value of 0.2 was applied for each of the FMO1, FMO3 and FMO5 isoform and for all other compounds. This optimized rFMO scalar also resulted in better predictions of observed PK profiles (Figure 3) with an increased correlation value (r^2) for the correlation of predicted versus observed clearance as shown in Figure 4. The Forest plot showing the

model performance using rFMO data of FMO substrates with and without scalar for all compounds are summarized in Supplementary Figure 1. The results of PK parameters for these two options are shown in Supplementary Table 3.

Discussion

The prediction of human PK properties can be critical for decision making when ranking short listed compounds, the assessment of lead series and for clinical drug candidates. A 'bottom-up' PBPK modelling approach involves modeling of the mechanisms of the drug disposition processes and simulating the human PK profiles by accounting for variability arising from enzyme expression at patient-level. The application of 'bottom-up' models depends on the availability of quality data and established IVIVE factors and scalars. Human PK predictions using PBPK models and data from in vitro assays such as hepatocytes or HLM CLint combined with the appropriate scalars appears to be robust for CYP enzymes (Wagner et al., 2015; Luzon et al., 2016). However, very limited knowledge of scaling factors exists for drugs that are metabolized by non-CYPs such as FMOs. As a result, early bottom-up models will require verification with in vivo clinical data, and in some cases calibration of parameters including scaling factors through a 'middle-out' approach (i.e., combining clinical data and in-vitro data) in order to be considered to be more impactful in the drug development process. A method that many consider would provide greater certainty is to compare the predictions from two or more methods. An example would be comparing two predictions based upon the same input data set, in this case comparing the results shown in the earlier paper Jones et al, 2017 vs the PBPK modelling approach.

In this paper, we use a PBPK M&S approach to predict the PK parameters, to verify and simulate the observed clinical data of FMO substrates and compare with our earlier IVIVE results (Jones et al., 2017). Human hepatocytes produced a good concordance (R^2=0.72) between the predicted and observed in vivo clearance values (Figure. 4), while all drugs fell within 2-fold. The correlation between predicted and observed in vivo clearance was weaker for HLM and rFMO which is consistent with our earlier study (Jones et al., 2017).

The PBPK results using rFMO in vitro data deviated from the observed exposure by approximately 2.5-fold, when a scalar of zero is used. This biased prediction may not be surprising, as individual rFMO and HLM scaling factors are required to compensate for differences in the intrinsic activity per unit enzyme of rFMO relative to HLM. The observed clinical data can be used to refine and/or improve the model performance via a 'middle-out' approach (combination of top-down and bottom-up approaches). We estimated a scaling factor to convert enzyme kinetic values obtained in different expression systems to the equivalent in HLM.

This rFMO scalar concept is well established for rCYPs within PBPK platforms such as Simcyp and shown to be applicable for rUGTs as well (Lin, 2015). In addition to a compound specific ISEF (Supplementary Table 1), an attempt was made to generate a tissue specific scalar similar to that which exists for UGT enzymes within simulator. In order to determine the scalar value associated with a particular rFMO isoform we performed a sensitivity analysis and parameter estimation analysis using itopride clinical data (Figure 4). The ASA approach suggested that an rFMO scalar value of around 0.2 is required to recover the itopride clinical data. This rFMO scalar of 0.2 also resulted in better predictions for other compounds as shown in Figure 3, or Supplementary Figure 1 than when the rFMO scalar of zero is used. This analysis shows that the observed data can be used to refine the model performance via fitting the clinical data to estimate a few of the model parameters in this case the rFMO scalar to improve the model's predictive performance of other FMO substrates using data of corresponding rFMO in vitro assay.

When developing the model based on the rFMO data the elimination via FMO1, FMO3, FMO5 were considered separately along with respective liver, kidney and intestine expression levels. The intrinsic catalytic activity per unit amount of FMO1, FMO3 and FMO5 enzymes were 71 pmol/mg protein in liver, 47 pmol/mg protein in kidney and 22 pmol/mg protein in intestine to reflect the abundances of FMO3, FMO1 and FMO5, respectively were included in the population file. The impact of FMO3 polymorphisms was included in the final PBPK model.

DMD Fast Forward. Published on June 12, 2018 as DOI: 10.1124/dmd.118.080648
This article has not been copyedited and formatted. The final version may differ from this version.

PBPK model approaches allow the simulation of PK profiles by taking account of parameter uncertainty. This uncertainty reflects both uncertainty in the experimental values of input parameters into a model along with variability arising from FMO expression and demographics. This is unlike simple IVIVE methods that do not take variability arising from expression, demographics and experimental errors into account (Jones et al., 2017). Thus, the correlation values from PBPK modelling gives more confidence in the scaling approach on top of simple IVIVE methods.

Once the PBPK model is verified it can be applied to predict the drug exposure differences in subjects with FMO3 wild type and homozygous FMO Lys158/Gly308 mutant genotypes as shown by Zhou et al (Zhou et al., 2017) for itopride. In addition, we can apply the developed PBPK model to special populations like paediatrics, as FMO abundance data recently quantified will allow accounting for an ontogeny.

The ontogeny of hepatic FMO exhibits a similar trend to the CYP3A family, where FMO1 resembles the pattern of CYP3A7 and FMO1 and FMO3 expression data has been quantified using a HLM system (Koukouritaki et al., 2002). Moreover, it was shown that FMO3 matures to the adult level by 10 years of age (Hines and McCarver, 2002; Koukouritaki et al., 2002), requiring a dose adjustment because of this ontogeny process. Currently, the paediatric clinical data for FMO substrates is lacking, but a prospective simulation for itopride across the age range from 6 months to 12 years of age is shown in Supplementary Table 4.

Our results confirm that clearance by FMO in human can be assessed and de-risked using a set of in vitro DMPK assays. When combined with physiological-based pharmacokinetic modelling, it allows for more robust prediction of AUC and other PK parameters further supporting de-risking during the drug development process.

Acknowledgements

The authors wish to thank Andy Sykes, Helen Humphries, Iain Gardner, and Sibylle Neuhofff for their scientific input in carrying out the PBPK analyses described in this paper.

Authorship Contributions

Participated in research design: Pilla Reddy, Jones, and Colclough

Conducted experiments: Srivastava, Wilson and Li

Performed data analysis: Pilla Reddy and Jones

Wrote or contributed to the writing of the manuscript: Pilla Reddy, Jones, Srivastava, Colclough, Wilson, and Li

References

Albers LJ, Reist C, Vu RL, Fujimoto K, Ozdemir V, Helmeste D, Poland R, and Tang SW (2000) Effect of venlafaxine on imipramine metabolism. *Psychiatry Res* **96:**235-243.

Baldock GA, Brodie RR, Chasseaud LF, Taylor T, Walmsley LM, and Catanese B (1991) Pharmacokinetics of benzydamine after intravenous, oral, and topical doses to human subjects. *Biopharm Drug Dispos* **12:**481-492.

Brosen K and Gram LF (1988) First-pass metabolism of imipramine and desipramine: impact of the sparteine oxidation phenotype. *Clin Pharmacol Ther* **43:**400-406.

Cashman JR and Zhang J (2006) Human flavin-containing monooxygenases. *Annu Rev Pharmacol Toxicol* **46:**65-100.

Chen Y, Zane NR, Thakker DR, and Wang MZ (2016) Quantification of Flavin-containing Monooxygenases 1, 3, and 5 in Human Liver Microsomes by UPLC-MRM-Based Targeted Quantitative Proteomics and Its Application to the Study of Ontogeny. *Drug Metab Dispos* **44:**975-983.

Chiu CC, Lane HY, Huang MC, Liu HC, Jann MW, Hon YY, Chang WH, and Lu ML (2004) Dose-dependent alternations in the pharmacokinetics of olanzapine during coadministration of fluvoxamine in patients with schizophrenia. *J Clin Pharmacol* **44:**1385-1390.

Dolphin CT, Cullingford TE, Shephard EA, Smith RL, and Phillips IR (1996) Differential developmental and tissue-specific regulation of expression of the genes encoding three members of the flavin-containing monooxygenase family of man, FMO1, FMO3 and FM04. *Eur J Biochem* **235:**683-689.

Elshafeey AH, Elsherbiny MA, and Fathallah MM (2009) A single-dose, randomized, two-way crossover study comparing two olanzapine tablet products in healthy adult male volunteers under fasting conditions. *Clin Ther* **31:**600-608.

Fuchs WS, Leary WP, van der Meer MJ, Gay S, Witschital K, and von Nieciecki A (1996) Pharmacokinetics and bioavailability of tamoxifen in postmenopausal healthy women. *Arzneimittelforschung* **46:**418-422.

Ganaton (2017) Ganaton Japanese Label. http://www.meppo.com/pdf/drugs/2845-GANATON-1415104080.pdf.

Garg DC, Eshelman FN, and Weidler DJ (1985) Pharmacokinetics of ranitidine following oral administration with ascending doses and with multiple-fixed doses. *J Clin Pharmacol* **25:**437-443.

Haining RL, Hunter AP, Sadeque AJ, Philpot RM, and Rettie AE (1997) Baculovirus-mediated expression and purification of human FMO3: catalytic, immunochemical, and structural characterization. *Drug Metab Dispos* **25:**790-797.

Hines RN and McCarver DG (2002) The ontogeny of human drug-metabolizing enzymes: phase I oxidative enzymes. *J Pharmacol Exp Ther* **300:**355-360.

Humphries H, Neuhoff S, and Gardner I (2015) Application of PBPK Modelling for Prediction of FMO Metabolism Using Benzydamine as a Probe for FMO3. . *44th DMDG Open Meeting, Cambridge UK*.

Jamei M, Marciniak S, Edwards D, Wragg K, Feng K, Barnett A, and Rostami-Hodjegan A (2013) The simcyp population based simulator: architecture, implementation, and quality assurance. *In Silico Pharmacol* **1:**9.

Jones BC, Srivastava A, Colclough N, Wilson J, Reddy VP, Amberntsson S, and Li D (2017) An Investigation into the Prediction of in Vivo Clearance for a Range of Flavin-containing Monooxygenase Substrates. *Drug Metab Dispos* **45:**1060-1067.

Katagiri F, Shiga T, Inoue S, Sato Y, Itoh H, and Takeyama M (2006) Effects of itopride hydrochloride on plasma gut-regulatory peptide and stress-related hormone levels in healthy human subjects. *Pharmacology* **77:**115-121.

Koukouritaki SB and Hines RN (2005) Flavin-containing monooxygenase genetic polymorphism: impact on chemical metabolism and drug development. *Pharmacogenomics* **6:**807-822.

Koukouritaki SB, Simpson P, Yeung CK, Rettie AE, and Hines RN (2002) Human hepatic flavin-containing monooxygenases 1 (FMO1) and 3 (FMO3) developmental expression. *Pediatr Res* **51:**236-243.

Lin J (2015) In-vitro-in-vivo extraploation of UGT1A9-mediated clerance and application in a PBPK model for dapagliflozin. *44th DMDG Open Meeting, Cambridge UK*.

Luzon E, Blake K, Cole S, Nordmark A, Versantvoort C, and Berglund EG (2016) Physiologically based pharmacokinetic modeling in regulatory decision-making at the European Medicines Agency. *Clin Pharmacol Ther*.

McNeil JJ, Mihaly GW, Anderson A, Marshall AW, Smallwood RA, and Louis WJ (1981) Pharmacokinetics of the H2- receptor antagonist ranitidine in man. *Br J Clin Pharmacol* **12:**411-415.

NCT02093351 (2017) To Assess Safety and Effect of Olaparib on the Pharmacokinetics of Anastrozole, Letrozole & Tamoxifen, and Their Effect on Olaparib, in Patients With Advanced Solid Cancer.

Nguyen HQ, Callegari E, and Obach RS (2016) The Use of In Vitro Data and Physiologically-Based Pharmacokinetic Modeling to Predict Drug Metabolite Exposure: Desipramine Exposure in Cytochrome P4502D6 Extensive and Poor Metabolizers Following Administration of Imipramine. *Drug Metab Dispos* **44:**1569-1578.

Obach RS, Baxter JG, Liston TE, Silber BM, Jones BC, MacIntyre F, Rance DJ, and Wastall P (1997) The prediction of human pharmacokinetic parameters from preclinical and in vitro metabolism data. *J Pharmacol Exp Ther* **283:**46-58.

Overby LH, Carver GC, and Philpot RM (1997) Quantitation and kinetic properties of hepatic microsomal and recombinant flavin-containing monooxygenases 3 and 5 from humans. *Chem Biol Interact* **106:**29-45.

Raaflaub J, Haefelfinger P, and Trautmann KH (1984) Single-dose pharmacokinetics of the MAO-inhibitor moclobemide in man. *Arzneimittelforschung* **34:**80-82.

Reddy RR, Ralph EC, Motika MS, Zhang J, and Cashman JR (2010) Characterization of human flavin-containing monooxygenase (FMO) 3 and FMO5 expressed as maltose-binding protein fusions. *Drug Metab Dispos* **38:**2239-2245.

Rodgers T, Leahy D, and Rowland M (2005) Physiologically based pharmacokinetic modeling 1: predicting the tissue distribution of moderate-to-strong bases. *J Pharm Sci* **94:**1259-1276.

Rodgers T and Rowland M (2006) Physiologically based pharmacokinetic modelling 2: predicting the tissue distribution of acids, very weak bases, neutrals and zwitterions. *J Pharm Sci* **95:**1238-1257.

Schoerlin MP, Mayersohn M, Korn A, and Eggers H (1987) Disposition kinetics of moclobemide, a monoamine oxidase-A enzyme inhibitor: single and multiple dosing in normal subjects. *Clin Pharmacol Ther* **42:**395-404.

Sjogren E, Westergren J, Grant I, Hanisch G, Lindfors L, Lennernas H, Abrahamsson B, and Tannergren C (2013) In silico predictions of gastrointestinal drug absorption in pharmaceutical product development: application of the mechanistic absorption model GI-Sim. *Eur J Pharm Sci* **49:**679-698.

Takano A, Suhara T, Kusumi I, Takahashi Y, Asai Y, Yasuno F, Ichimiya T, Inoue M, Sudo Y, and Koyama T (2006) Time course of dopamine D2 receptor occupancy by clozapine with medium and high plasma concentrations. *Prog Neuropsychopharmacol Biol Psychiatry* **30:**75-81.

Taniguchi-Takizawa T, Shimizu M, Kume T, and Yamazaki H (2015) Benzydamine N-oxygenation as an index for flavin-containing monooxygenase activity and benzydamine N-demethylation by cytochrome P450 enzymes in liver microsomes from rats, dogs, monkeys, and humans. *Drug Metab Pharmacokinet* **30:**64-69.

Tassaneeyakul W, Kittiwattanagul K, Vannaprasaht S, Kampan J, Tawalee A, Puapairoj P, Tiamkao S, Juthagridsada S, Kukongviriyapan V, and Tassaneeyakul W (2005) Steady-state bioequivalence study of clozapine tablet in schizophrenic patients. *J Pharm Pharm Sci* **8:**47-53.

Traynor AM, Hewitt M, Liu G, Flaherty KT, Clark J, Freedman SJ, Scott BB, Leighton AM, Watson PA, Zhao B, O'Dwyer PJ, and Wilding G (2011) Phase I dose escalation study of MK-0457, a novel Aurora kinase inhibitor, in adult patients with advanced solid tumors. *Cancer Chemother Pharmacol* **67:**305-314.

Wagner C, Zhao P, Pan Y, Hsu V, Grillo J, Huang SM, and Sinha V (2015) Application of Physiologically Based Pharmacokinetic (PBPK) Modeling to Support Dose Selection: Report of an FDA Public Workshop on PBPK. *CPT Pharmacometrics Syst Pharmacol* **4:**226-230.

Yeung CK, Lang DH, Thummel KE, and Rettie AE (2000) Immunoquantitation of FMO1 in human liver, kidney, and intestine. *Drug Metab Dispos* **28:**1107-1111.

Yoon S, Lee H, Kim TE, Lee S, Chee DH, Cho JY, Yu KS, and Jang IJ (2014) Comparative steady-state pharmacokinetic study of an extended-release formulation of itopride and its immediate-release reference formulation in healthy volunteers. *Drug Des Devel Ther* **8:**123-128.

Zhou W, Humphries H, Neuhoff S, Gardner I, Masson E, Al-Huniti N, and Zhou D (2017) Development of a physiologically based pharmacokinetic model to predict the effects of flavin-containing monooxygenase 3 (FMO3) polymorphisms on itopride exposure. *Biopharm Drug Dispos* **38:**389-393.

Legend for Figures

Figure 1. Mean simulated using hepatocyte CLint data (solid line) and observed (data points) concentrations of FMO substrates after administration of a single dose to humans for 9 FMO substrates. The grey lines around the solid black line represent simulated individual trials matched to a clinical study. Lower and upper grey lines represent the 90% confidence interval of the respective simulations.

Figure 2. Forest plot showing the physiologically based pharmacokinetic modeling performance of FMO substrates. Predictions are expressed as ratios of predicted over observed of area under the curve (AUC). The dashed line represents the identity (predicted/observed ratio), and the gray shade represents the 0.5–2.0 ratio window and blue shaded area represents 0.67-1.50-fold ratio. Mean AUC using hepatocytes (blue squares); Mean AUC using HLM (red circles); Mean AUC using rFMO with no scaling (green triangles) with error bars represented as percentile range (5^{th} and 95^{th} percentile).

Figure 3. Determination of rFMO scalar for itopride and its application to tozasertib as an example. Figures 3A, 3B, 3C shows the model fit without rFMO scalar, with rFMO tissue scalar and with rFMO ISEF scalar for itopride, respectively and Figures 3D, 3E, 3F shows the tozasertib model without rFMO scalar, with rFMO tissue scalar and with rFMO ISEF scalar, respectively.

Figure 4. Correlations for PBPK model predicted clearance using human hepatocytes, HLM, and rFMO with ISEF scalar and tissue specific scalar.

Table 1: Clinical data used for PBPK model verification

Drug	Age range (yrs)	Number of subject	Male/Female numbers	Dose (route)	Dosage Regimen/ PK Duration	Comments	Reference
Benzydamine	41~51	6	6/0	5 mg, IV	Single/48hrs	Caucasian Healthy volunteers	(Humphries et al., 2015)
	18~51	12	6/6	50 mg, oral	Single/48hr	Caucasian Healthy volunteers	
Itopride	-	6	6/0	50 mg, oral	Single/24hr	Japanese Healthy volunteers	(Yoon et al., 2014)
	24~31	5	5/0	150 mg, oral	Single/24hr	Japanese Healthy volunteers	(Katagiri et al., 2006)
Tozasertib	22~80	27	14/13	4, 8,16,32,45,64 & 96 mg/m^2 IV	Single, 24hr infusion	Oncology Patients	(Traynor et al., 2011)
Tamoxifen	29~71	29	4/25	20 mg, Oral	Multiple, PK at SS	Oncology Patients	AZ internal data (NCT02093351, 2017)
	41~64	24	0/24	30 mg, Oral	Single	Healthy volunteers	(Fuchs et al., 1996)
Moclobemide	21~30	12	12/0	150 mg, IV, 20 min infusion	Single	Healthy volunteers	(Raaflaub et al., 1984)
	21~30	12	12/0	100 mg, Oral	Single	Healthy volunteers	(Schoerlin et al., 1987)
Imipramine	23~64	8	8/0	100 mg, Oral	Single	Caucasian Healthy volunteers	(Albers et al., 2000)
	22~37	11	5/6	50 mg, IV 100 mg, PO	Single	Caucasian Healthy volunteers	(Brosen and Gram, 1988)
Clozapine	21~30	18	18/0	100 mg; BID, oral	Single	Asian Healthy volunteers	(Tassaneeyakul et al., 2005)
	30~32	2	2/0	200 and 600 mg, oral	Multiple, PK at SS	Caucasian Schizophrenic Patients	(Takano et al., 2006)

Olanzapine	28~50	10	10/0	10 mg, oral	Single	Schizophrenic Patients	(Elshafeey et al., 2009)
	19~41	24	24/0	10 mg, oral	Single	Healthy volunteers	(Chiu et al., 2004)
Ranitidine	21~23	6	6/0	20 mg IV and 100 mg oral	Single	Healthy volunteers	(McNeil et al., 1981)
	19~32	12	12/0	100 to 400 mg Oral	Single and multiple	Healthy volunteers	(Garg et al., 1985)

PO: Per oral; IV Intravenous; SS: Steady-state; QD: once daily, BID: Twice daily

Table 2: PBPK Model Input Parameters

Parameter	Description	Unit	Parameter Value								
Physicochemical data (source: AstraZeneca experimental data) (Jones et al., 2017)			**Benzydamine**	**Itopride**	**Tozasertib**	**Tamoxifen**	**Moclobemide**	**Imipramine**	**Clozapine**	**Olanzapine**	**Ranitidine**
MW	Molecule weight	g/mol	309.4	358.4	464.6	371.5	268.7	280.4	326.8	312.4	314.4
log P/log D	Octanol: buffer partition coefficient		4.24/2.34	2.12/0.72	4.3/3.36	6.8/4.62	2.17/1.65	5.03/4.51	3.5/2.96	3.5/2.15	0.67/-0.78
pKa/type	dissociation constant		9.3/Base	8.8/ Base	8.3/ Base	8.8/Base	6/ Base	9.4/ Base	Base	7.2/ Base	8.2/2.7Diprotic Base
BP	Blood-to-plasma partition ratio		0.76	0.72	0.94	0.89	0.84	0.93	0.825	0.73	0.90
Fu	Fraction unbound in plasma		0.146	0.262	0.0873	0.00035	0.638	0.261	0.0925	0.327	0.912
Absorption											
Ka	Absorption rate constant	1/h	1.21	4, lag time of 0.4 h	-	0.39	1.12	1	2.2.2	1.36	0.38
Fugut	Unbound fraction of drug in gut enterocytes. Either default of 1 or predicted value used		1	0.192	1	1	1	1	1	1	1
Pcaco-2	Caco-2 permeability	$\times 10^{-6}$ cm/s	Mech-eff model	-	-	Mech-eff model	64.4	Mech-eff model	PSA/HBD	PSA/HBD	PSA/HBD
Peff,man	Human jejunum permeability	$\times 10^{-4}$ cm/s	8.71	5	-	4.09	6.95	8.56	7.87	7.83	0.94
Distribution											
Vss	Distribution volume at steady-state after IV or predicted using Method 2	L/Kg	0.966	6.3	5.6	15.7	3.59	17.1	1.6	5.1	1.50
	Distribution model		Minimal PBPK model	Full PBPK	Full PBPK	Full PBPK	Full PBPK	Minimal PBPK	Minimal PBPK	Minimal PBPK	Full PBPK
Elimination											
Clint-HLM	Human liver microsomal protein in vitro intrinsic clearance	µL/min/mg protein	18	18	61	4	3	14	18	<3	<3

Clint-Hepatocytes	Hepatocytes in vitro intrinsic clearance	µL/min/10^6 cells	9	11	29	4	3	9	5	2	0.6
Fm (% FMO) contribution		%	53	96	38	28	38	21	23	23	26

CLint - rFMO	FMO in-vitro intrinsic clearance and remaining metabolic CL was accounted via major metabolizing enzyme via HLM in enzyme kinetics or via rCYP if CYP contribution known	µL/min/ pmol protein or µL/min/ mg protein for HLM	FMO1=0.44 FMO3=0.29 FMO5=0.001 CYP2D6=8.5	FMO1=0.79 FMO3=0.118 FMO5=0.0.052 CYP3A4=0.87	FMO1=0.24 FMO3=0.48 FMO5=0 CYP3A4=39	FMO1=0.083 FMO3=0 FMO5=0 CYP3A4= 3.6	FMO1=0.018 FMO3=0.031 FMO5=0.003 CYP3A4=2.9	FMO1=0.163 FMO3=0.013 FMO5=0.001 CYP1A2=0.058 2C19 2.36 2D6 =47 3A4=0.021 Additional HLM CL=1.52	FMO1=0.031 FMO3=0 FMO5=0 CYP3A4=11.1	FMO1=0.04 FMO3=0.006 FMO5=0 CYP3A4=2.31	FMO1=0.011 FMO3=0.003 FMO5=0.028 CYP3A4=2.22
Systemic clearance	Systemic absolute CL or oral CL	L/h	9.66[a]	88[b]	87[a]	8[b]	63.7[a]	54[b]	32[b]	26[b]	7.56[a]
Renal clearance	Renal CL	L/h	0.24	1.5	-	-	-	-	-	-	24.6
Fumic	Unfound fraction in microsomes		0.35	1.05	0.18	0.02	0.98	0.31	0.30	0.73	0.97
Fuinc	Unfound fraction in hepatocytes		0.74	0.88	0.21	0.003	0.87	0.65	0.33	0.86	0.98

CYP, Cytochrome P450; CL, clearance; CLint, intrinsic clearance; FMO, flavin-containing monooxygenases; Fm, fraction metabolized; HLM, human liver microsomes; rFMO, recombinant FMO; rCYP, recombinant Cytochrome P450; PBPK, Physiologically based pharmacokinetic; PK Pharmacokinetics. Vss, volume of distribution at steady state; PSA, polar surface area; HBD, Hydrogen bond donor; [a] from intravenous study using references shown in Table 3 for a respective drug; [b] from oral study using references shown in Table 3 for a respective drug.

Table 3: Observed mean PK parameters for FMO substrates using hepatocyte data

Drug	Dosing Regimen	Dose (mg)	Obs. AUC [ng*h/ml] (SD)	Obs. Cmax [ng/ml] (SD)	Obs. CL [L/h] (SD)	Pred. AUC with Heps [ng*h/ml]	Pred. Cmax with Heps [ng/ml]	Pred. CL [L/h] (SD)	Reference for the observed data
Benzydamine	IV	5	540 (112)	68 (19)	9.6	594 (191)	74 (18)	8.89 (3.2)	(Baldock et al., 1991)
	PO	50	4994 (1190)	546 (177)	9.8	4245 (1748)	398 (126)	9.4 (3.2)	(Baldock et al., 1991)
Itopride	PO	50	750 (123)	280 (49)	-	1440 (424)	353 (61)	37.6 (11)	(Ganaton, 2017)
	PO	150	2170 (349)	930 (50)	55-88	1940 (442)[&]	1061 (184)	81 (18)	(Katagiri et al., 2006)
Tozasertib	IV	4212	77673 (18560)	3547 (1113)	53.6 (17.6)	85135 (20883)	3480 (797)	47 (11)	(Traynor et al., 2011)
Tamoxifen	PO (multiple dose)	20	2336 (699)	134.8 (35.5)	7.68 (2.2)	1938 (488)	94 (22)	11 (4)	(NCT02093351, 2017)
	PO	30	3370 (701)	63.6 (11.1)	NR	2379 (580)	58 (15)	14 (4)	(Fuchs et al., 1996)
Moclobemide	IV	150	3807	2100	39.4 (5.9)	4180 (738)	3825 (376)	36(6)	(Raaflaub et al., 1984)
	PO	100	1570	823	63.7	1859 (459)	531 (138)	57 (18)	(Schoerlin et al., 1987)
Imipramine	IV	1	28 (12-22)	(0.35 to 0.60)	39.5 (33.6-63)	16 (4)	0.9 (0.3)	65 (13)	(Nguyen et al., 2016)
	PO	100	985 (662)	63.2 (40)	126 (88)	1663 (614)	46 (17)	69 (28)	(Albers et al., 2000)
Clozapine	PO	100	3994 (2144)	185 (132)	31.81 (16)	5465 (2097)	493 (179)	21 (9)	(Tassaneeyakul et al., 2005)
Olanzapine	PO	10	823 (480) AUC0-120h	21.4 (14)	13 (4.6)	623 (197)	20 (6)	18 (7)	(Chiu et al., 2004)

Ranitidine	IV	20	488 (40)	615	43 (3.7)	470 (99)	891 (108)	49 (14)	(McNeil et al., 1981)
	PO	100	1726 (418)	342 (122)	-	1551 (388)	280 (48)	68 (17)	

*Cmax = conc. at end of infusion, & AUC (0-4hr) to match the reported AUC; PO: Per oral; IV Intravenous; SS: Steady-state; QD: once daily, BID: Twice daily; heps, hepatocytes; SD: standard deviation; NR= not reported

DMD Fast Forward. Published on June 12, 2018 as DOI: 10.1124/dmd.118.080648
This article has not been copyedited and formatted. The final version may differ from this version.

Figure 1.

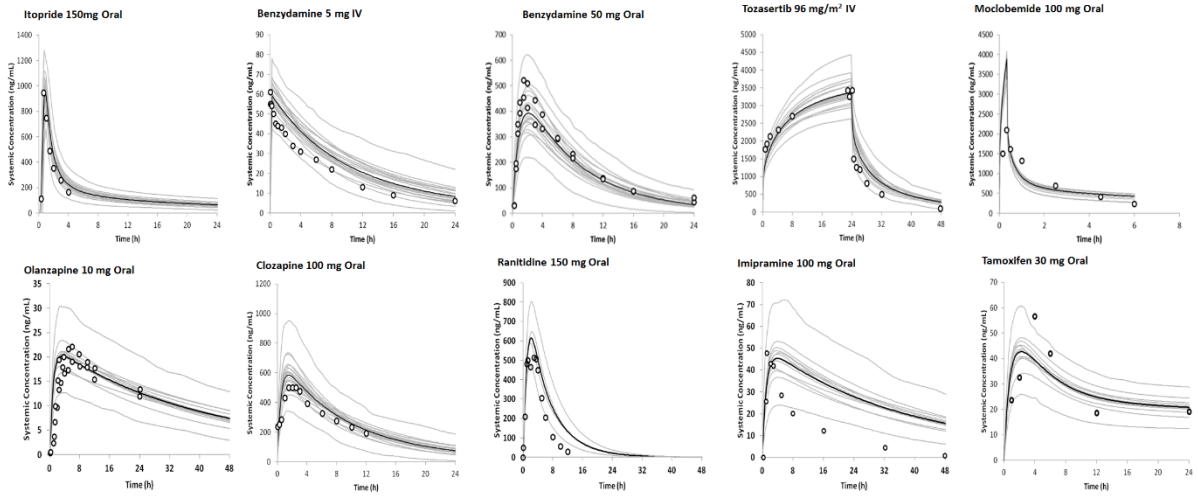

DMD Fast Forward. Published on June 12, 2018 as DOI: 10.1124/dmd.118.080648
This article has not been copyedited and formatted. The final version may differ from this version.

Figure 2.

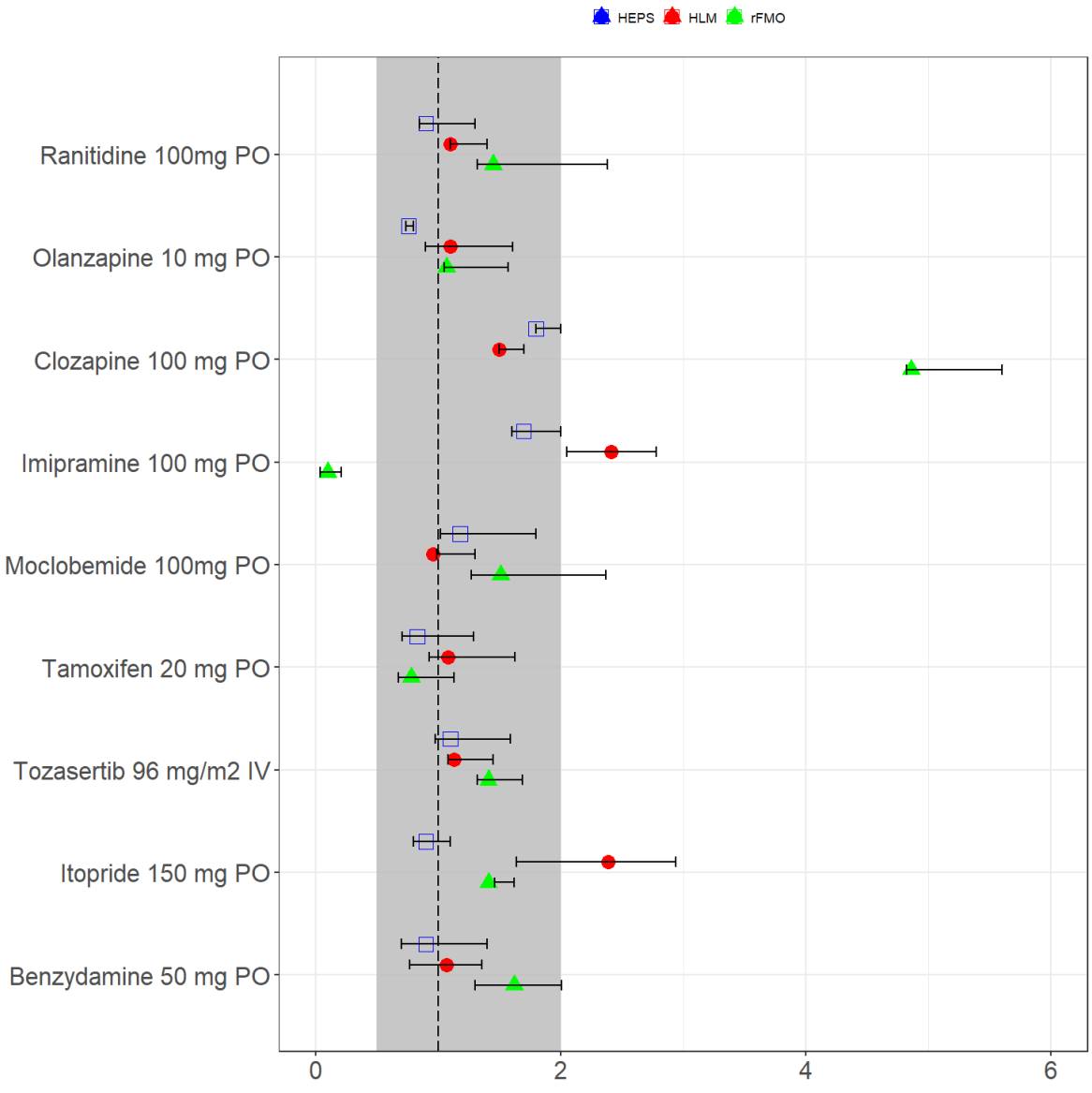

DMD Fast Forward. Published on June 12, 2018 as DOI: 10.1124/dmd.118.080648
This article has not been copyedited and formatted. The final version may differ from this version.

Figure 3.

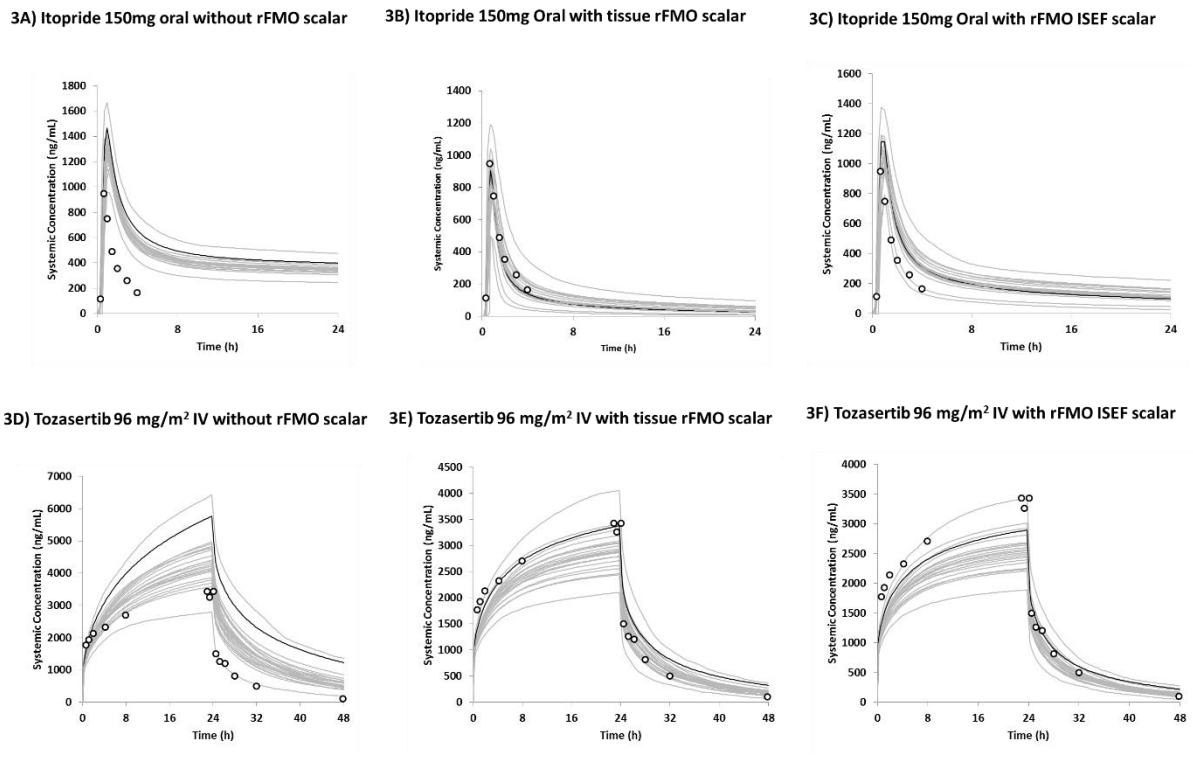

DMD Fast Forward. Published on June 12, 2018 as DOI: 10.1124/dmd.118.080648
This article has not been copyedited and formatted. The final version may differ from this version.

Figure 4.

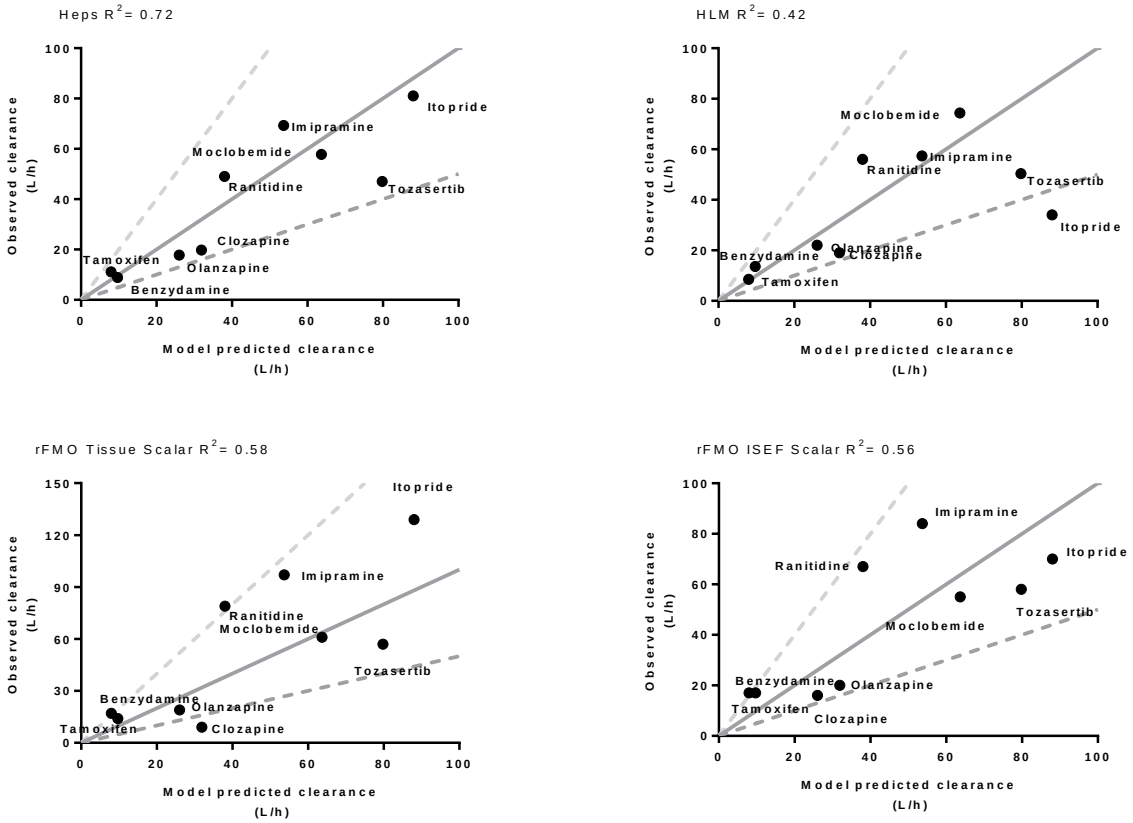

Supplemental Material for

Drug Metabolism and Disposition

An investigation into the prediction of the plasma concentration-time profile and its inter-individual variability for a range of flavin-containing monooxygenase substrates using a mechanistic physiologically based pharmacokinetic modelling approach

Venkatesh Pilla Reddy, Barry C Jones, Abhishek Srivastava Nicola Colclough, Joanne Wilson, and Danxi Li

Supplementary Table 1: Human *in vitro* data for FMO substrates (Jones et al., 2017)

	Human hepatocytes				Human liver microsomes				rFMO						Fm (% FMO) contribution
	Clint (µl/min/10^6 cells)	Fu inc[a]	Predicted Clint u (ml/min/kg)	Predicted Clearance (ml/min/kg)	Clint (µl/min/mg)	Fu mic	Predicted Clint u (ml/min/kg)	Predicted Clearance (ml/min/kg)	Clint (µl/min/pmol) with [ISEF]			Clint (µl/min/mg)[c]			
									FMO1	FMO3	FMO5	FMO1	FMO3	FMO5	
Benzydamine	9	0.74	104	11	18	0.35	148	13	0.435 [0.9]	0.288 [0.9]	0.001 [>100]	261	92	1	53
Imipramine	9	0.65	122	13	14	0.31	129	13	0.163 [1.6]	0.013 [13.6]	0.001 [>100]	98	4	2	21
Olanzapine	2	0.86	18	5	<3[b]	0.73	12	4	0.036 [1.8]	0.005 [9.4]	-	21	1	-	23[#]
Ranitidine	0.6*	0.98	5	4	<3[b]	0.97	9	6	0.011 [5.6]	0.003 [14.5]	0.028 [5]	7	1	47	26[#]
Moclobemide	3	0.87	30	11	3	0.98	9	5	0.018 [5.6]	0.031 [2.1]	0.003 [71]	11	10	5	38
Itopride	11	0.88	107	14	18	1.05	49	10	0.340 [1.4]	0.497 [0.6]	-	204	159	-	96
Clozapine	5	0.33	131	10	18	0.30	173	11	0.031 [9.9]	-	-	18	-	-	23
Tamoxifen	4	0.003	9706	3	4	0.02	662	0.2	0.083 [1.4]	-	-	50	-	-	28[#]
Tozasertib	29	0.21	1177	19	61	0.18	971	18	0.244 [5.6]	0.481 [1.9]	0.0004 [>100]	146	154	1	38

All data n = 3 except for data marked with * which is n = 2; [a] Data from rat hepatocytes; [b] Value of 3µl/min/mg used in calculations

**ISEF calculated using formula for each isoform= $ISEF = \frac{CLint,u\ in\ HLM\ (\frac{ul}{min}) \Big/ HLM\ FMO\ abundance\ (\frac{pmol}{mg})}{CLint,u\ in\ rFMO\ (\frac{ul}{min}/pmol)}$

[#] It was not possible to determine the FMO contribution for ranitidine, olanzapine, and tamoxifen due to the low intrinsic clearance. However, an approximate FMO contribution was derived by fitting of the available rFMO CLint and FMO contribution data.

[c] Data was corrected for in-vitro FAD content.

Supplementary Table 2: Options used to define the elimination within PBPK platform (Simcyp V16)

Elimination option	Hepatocyte Data	In-Vitro HLM Data	In-Vitro rFMO Data
Option used	Whole organ metabolic clearance	Whole organ metabolic clearance or enzyme kinetics via HLM option to take into account of non-cyp mediated pathways	Enzyme kinetics data of rFMO was used. For remaining metabolic CL was added as a HLM CL
FMO expression assigned	Default, not linked to specific enzyme	Unused UGT used as an user defined option within Simcyp	Unused UGT used as an user defined option within Simcyp (see Itopride workspace) Scalar value (ISEF or tissue specific value was optimized for rFMO data A tutorial video (entitled Elimination Route UGT- Part 2) in the E-learning tab of the Consortium Members' area facility of Certara shows the utilization of unused UGT enzyme and linking it to the abundance in population and tissue (https://members.simcyp.com/) https://members.simcyp.com/account/elearning/stream/?id=fd410b95-4fff-42e4-ac4b-e01f04a9b13a

Supplementary Figure 1: Forest plot showing the physiologically based pharmacokinetic modeling performance of FMO substrates using rFMO data with and without scalar (tissue specific or ISEF) in the model

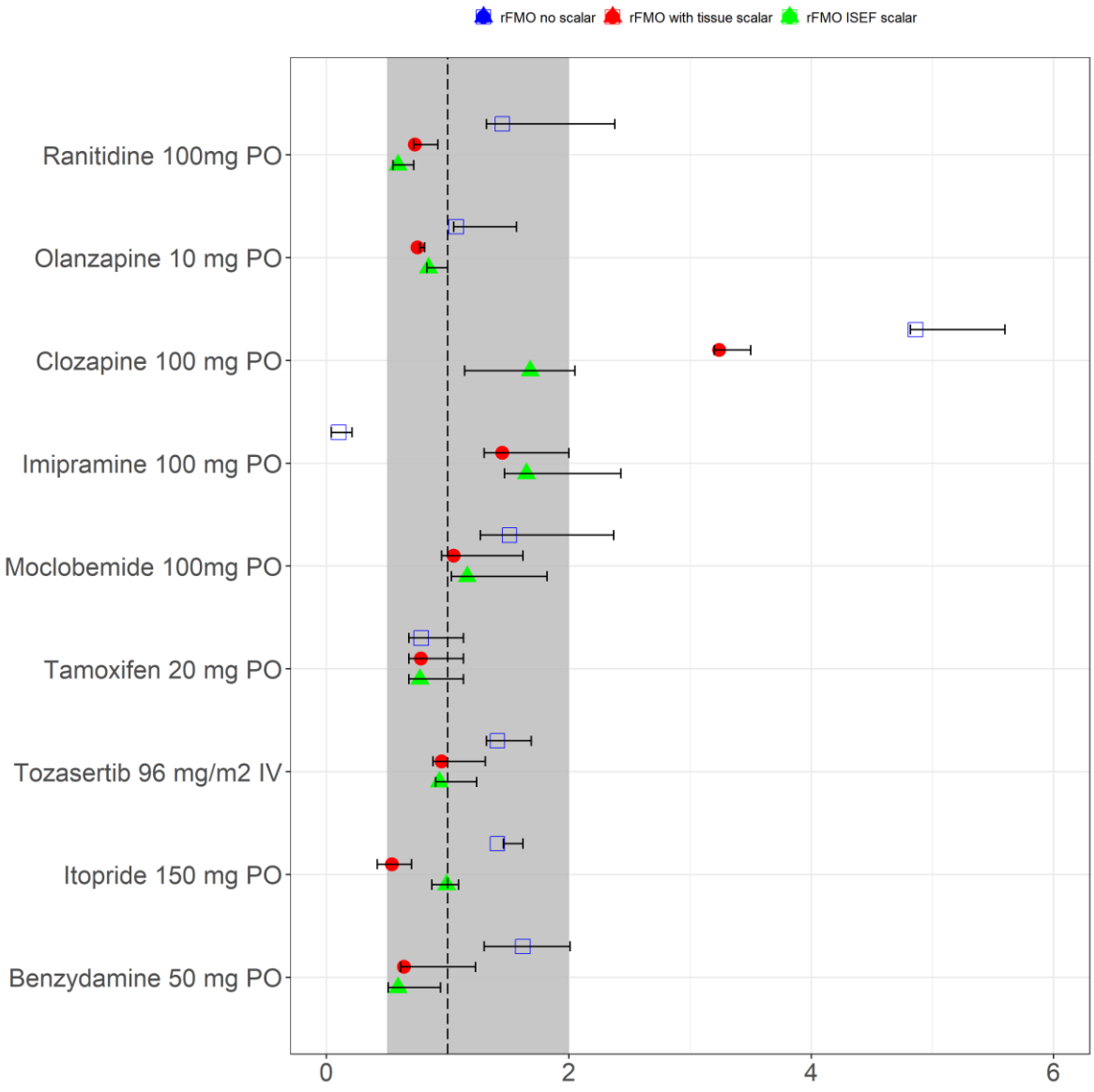

Supplementary Table 3: Simulated mean (SD) PK parameters for FMO substrates using HLM or rFMO with ISEF or tissue specific scalar data

Drug	Route	Dose (mg)	HLM			rFMO tissue scalar			rFMO ISEF scalar		
			AUC [ng*h/ml]	Cmax [ng/ml]	CL [L/h]	AUC [ng*h/ml]	Cmax [ng/ml]	CL [L/h]	AUC [ng*h/ml]	Cmax [ng/ml]	CL [L/h]
Benzydamine	PO	50	5329 (2411)	416 (135)	13 (6)	3441 (2296)	378 (135)	14 (9)	2931 (1720)	345 (126)	17 (11)
Itopride	PO	150	5192 (1840)	1090 (194)	34 (15)	1161 (395)	828 (175)	129 (56)	2142 (553)	1112 (201)	70 (25)
Tozasertib	IV	96	88109 (2088)	3480 (798)	50 (11)	73764 (17263)	2948 (674)	57 (12)	73763 (15474)	2888 (612)	58 (13)
Tamoxifen	PO	30	2521 (1579)	116 (27)	9 (3)	1831 (436)	42 (11)	17 (5)	1788 (437)	43 (11)	17 (5)
Moclobemide	PO	100	1509 (497)	417 (140)	74 (28)	1653 (437)	478 (124)	61 (18)	1822 (468)	499 (130)	55 (16)
Imipramine	PO	100	2021 (740)	51 (21)	57 (24)	1433 (810)	44 (21)	97 (12)	1625 (957)	46 (22)	84 (51)
Clozapine	PO	100	6080 (2487)	566 (216)	19 (8)	12931 (5195)	672 (233)	9 (6)	6698 (3252)	572 (212)	20 (14)
Olanzapine	PO	10	819 (226)	22 (6)	13 (4)	615 (210)	20 (6)	19 (8)	691 (224)	21 (6)	16 (6)
Ranitidine	PO	100	1960 (711)	366 (103)	56 (18)	1265 (628)	238 (97)	79 (42)	1024 (485)	207 (93)	67 (74)

*Cmax = conc. at end of infusion, [&] AUC (0-4hr) to match the reported AUC; PO: Per oral; IV Intravenous; SS: Steady-state; QD: once daily, BID: Twice daily; heps, hepatocytes; SD: standard deviation

Supplementary Table 4: Paediatrics simulations for Itopride using rFMO data

Age group	***FMO1 Expression****	***FMO3 Expression****	***Itopride dose, mg QD***	***Mean AUC (0-24), h·ng/mL***
Adults	1**	71±41 ***	150	2154
11–17 years	0.1±0.3	26.9±8.6	40	2435
10 months to 11 years	2.0±1.8	12.7±8.0	12	2281
3 weeks to <10 months	3.8±2.6	4.7±5.9	2.8	2006
0–3 weeks	7.8±5.3	1.1±3.3	1.4	2044

FMO expression data for age 0 to 17 years is from Koukouritaki et al., (Koukouritaki et al., 2002)

** (Cashman and Zhang, 2006)

*** (Haining et al., 1997; Overby et al., 1997)

Supplementary Table 5: Mass Spectrometer parameters for FMO substrates

Analyte	**MRM (Parent→Daughter) m/z**	**Dwell (s)**	**Cone voltage (V)**	**Collision energy (V)**
Tamoxifen	372.166→129.175	0.080	10	25
Moclobemide	269.053→182.073	0.080	10	15
Olanzapine	313.127→84.118	0.080	10	25
Imipramine	281.178→86.025	0.080	60	15
Tozasertib	465.195→190.215	0.080	20	40
Ranitidine	315.095→176.243	0.040	10	15
Benzydamine	310.173→86.065	0.080	60	30
Clozapine	327.14→270.16	0.080	40	20
Itopride	359.22→71.94	0.80	10	40
Verapamil (IS)	455.198→165.207	0.020	15	25

Supplementary Text:

LC-MS/MS analysis:

The concentration of all compounds in the incubations was determined by LC-MS/MS. An Acquity ultra performance liquid chromatography (UPLC) system, (Waters, UK) coupled to a triple-quadrupole mass spectrometer (Xevo TQ-S; Waters, Milford, MA) was used to carry out the sample analysis. The analytes were separated by reverse-phase liquid chromatography using a Waters Atlantis® T3, 3µm, 2.1X50mm column (Waters, UK). Mobile phases A and B consisted of water (containing 0.1% FA v/v) and ACN (containing 0.1% FA v/v), respectively. The flow rate was held constant at 0.73 ml/min throughout the gradient run. The initial mobile phase composition of 95% A and 5% B was held for 0.3 minutes. Mobile phase B was then increased linearly to 70% until 1.5 minutes, followed by further increase to 99% B until 1.59 minutes. At 1.6 minutes the composition of A and B was reversed to the initial 95% A and 5% B and was held until 2 minutes. Analyte quantitation was achieved by MS–MS detection in positive electrospray ionization mode. The MS operating conditions were as follows: the capillary voltage was 1.14 kV and source offset was 50 V. The desolvation temperature was set to 600 °C. Nitrogen was used as the desolvation gas (800 L/Hr) and cone gas (150 L/Hr). Argon was used as the collision gas at a flow rate of 0.15 ml/min. Detection of the ions was performed in the MRM mode using the transitions described in Supplementary Table 5. Peak integration and calibrations were performed using TargetLynx software (Version 4.1, Waters, Milford, MA).

References

Cashman JR and Zhang J (2006) Human flavin-containing monooxygenases. *Annu Rev Pharmacol Toxicol* **46:**65-100.

Haining RL, Hunter AP, Sadeque AJ, Philpot RM, and Rettie AE (1997) Baculovirus-mediated expression and purification of human FMO3: catalytic, immunochemical, and structural characterization. *Drug Metab Dispos* **25:**790-797.

Jones BC, Srivastava A, Colclough N, Wilson J, Reddy VP, Amberntsson S, and Li D (2017) An Investigation into the Prediction of in Vivo Clearance for a Range of Flavin-containing Monooxygenase Substrates. *Drug Metab Dispos* **45:**1060-1067.

Koukouritaki SB, Simpson P, Yeung CK, Rettie AE, and Hines RN (2002) Human hepatic flavin-containing monooxygenases 1 (FMO1) and 3 (FMO3) developmental expression. *Pediatr Res* **51:**236-243.

Overby LH, Carver GC, and Philpot RM (1997) Quantitation and kinetic properties of hepatic microsomal and recombinant flavin-containing monooxygenases 3 and 5 from humans. *Chem Biol Interact* **106:**29-45.